

A Wrist and Finger Force Sensor Module for Use During Movements of the Upper Limb in Chronic Hemiparetic Stroke

Laura C. Miller, Ricardo Ruiz-Torres, Arno H. A. Stienen, and Julius P. A. Dewald*, *Member, IEEE*

Abstract—Previous studies using robotic devices that focus on the wrist/fingers following stroke provide an incomplete picture of movement dysfunction because they do not consider the abnormal joint torque coupling that occurs during progressive shoulder abduction loading in the paretic upper limb. This letter introduces a device designed to measure isometric flexion/extension forces generated by the fingers, wrist, and thumb during robot-mediated 3-D dynamic movements of the upper limb. Validation data collected from eight participants with chronic hemiparetic stroke are presented in this paper.

Index Terms—Hand, kinetic measurements, robotic rehabilitation, shoulder loading, stroke, upper extremity.

I. INTRODUCTION

IN RECENT years, the quest for more effective rehabilitation strategies for the upper limb following hemiparetic stroke has focused on employing instrumented robotic devices to explore motor learning, to investigate the effects of treatment intensity, and to study mechanisms underlying stroke-induced movement disorders. This letter introduces a device, the Wrist/Finger Force Sensing module (WFFS), which is designed to quantify potential abnormal joint torque coupling between the shoulder and wrist/fingers in the paretic upper limb. The WFFS measures isometric flexion/extension forces generated by the wrist, fingers, and thumb during 3-D movements of the paretic upper limb.

In the paretic upper limb of moderately to severely affected hemiparetic stroke survivors, coupling between shoulder abductors and elbow, wrist and finger flexors, clinically described as the flexion synergy [1], [2], frequently occurs. This coupling could partially explain the hypertonia in the wrist/finger

flexors observed frequently during upper limb movements following stroke. Robotic assistive devices for the hand, such as extension-aiding gloves and exoskeletons, have the potential to improve hand function, as do robot-aided rehabilitation protocols that can involve sophisticated and precise active or passive mechanical manipulations of the hand/wrist. However, the expression of the stroke-induced flexion synergy at the hand must be better quantified before these technologies can reach their full potential.

Currently available robot assistive devices or robot-aided rehabilitation protocols for the hand and wrist are limited because they have examined the hand and wrist in isolation from the rest of the upper limb. Devices such as CyberGrasp exoskeleton (CyberGlove Systems), HandCARE [3], Rutgers Masters II [4], Hand-Wrist Assisting Robotic Device (HWARD) [5], Multiple User Virtual Environment for Rehabilitation (MUVER) [6], and other pneumatically controlled or actuated gloves [7], [8] are generally designed to assist hand opening, increase finger range of motion, or improve object grasp/release. Other devices, like the Haptic Knob [9], are designed to improve performance of functional tasks that require precise fine motor control. Similarly, studies that have used rotary actuators to quantify and to investigate the neural and mechanical mechanisms contributing to hand dysfunction, such as wrist/finger flexion/extension torques, reflex torques, and static and dynamic stiffness [10]–[16], are limited because the measurements have been taken while the rest of the upper limb was at rest. While the results from the aforementioned devices and studies are important for understanding the paretic hand, they cannot be generalized to 3-D movements of the whole limb.

The few robotic devices designed for whole-arm rehabilitation generally do not examine the effect that shoulder abduction (SABD) requirements may have on wrist/finger activity. The MIT-MANUS, with its new addition of a hand robot prototype [17], [18], and the Gentle/G system [19] train grasp and release movements in 3-D, but do so under gravity-compensated conditions only.

The advantage of simultaneous measurements from multiple upper limb joints during tasks performed with a varied amount of SABD loading has been illustrated by Beer *et al.* [20], Sukal *et al.* [21], and Ellis *et al.* [22]. Each study reported progressive reductions in active elbow extension for greater levels of SABD loading using either an air-bearing table [20] or the Arm Coordination Training 3-D robot (ACT^{3-D}) [21], [22] to vary the amount of SABD torque required to lift the limb and complete a task requiring elbow extension in the horizontal

Manuscript received February 2, 2009; revised May 4, 2009. First published June 26, 2009; current version published August 14, 2009. This work was supported in part by the National Institute on Disability and Rehabilitation Research (NIDRR) under Grant H133G070089. Asterisk indicates corresponding author.

L. C. Miller is with the Department of Biomedical Engineering and the Department of Physical Therapy and Human Movement Sciences, Northwestern University, Chicago, IL 60611 USA (e-mail: lcmiller@northwestern.edu).

R. Ruiz-Torres is with the Interdepartmental Neuroscience Program, Northwestern University, Chicago, IL 60611 USA (e-mail: ricardoruiz2013@u.northwestern.edu).

A. H. A. Stienen is with the Department of Physical Therapy and Human Movement Sciences, Northwestern University, Chicago, IL 60611 USA (e-mail: arnostienen@gmail.com).

*J. P. A. Dewald is with the Departments of Physical Therapy and Human Movement Sciences, Biomedical Engineering, Physical Medicine and Rehabilitation, and the Interdepartmental Neuroscience Program, Northwestern University, Chicago, IL 60611 USA (e-mail: j-dewald@northwestern.edu).

Digital Object Identifier 10.1109/TBME.2009.2026057

plane. These kinematic results can be explained by abnormal torque coupling between SABD and elbow flexion torques that have been measured under static conditions in earlier studies [23]–[25]. Despite the utility of these investigations, the potential abnormal wrist and finger torque coupling during generation of SABD torque has not been quantified.

Evaluating motor tasks completed during various levels of SABD loading can provide insight into the expression of the flexion synergy because descending synaptic drive is comodulated directly with the amount of required SABD. Several studies provide indirect evidence that increased descending synaptic drive causes a worsening of shoulder and elbow torque coupling that may be due to an increased influence of bulbospinal pathways following damage to corticospinal tracts [21], [22], [27], [28]. This hypothesis has been supported by studies that investigate the neural mechanisms contributing to reflex exaggerations in the paretic limb of stroke survivors, which have also provided results consistent with an increased influence of bulbospinal pathways [29], [30]. By measuring wrist/finger flexion/extension forces during 3-D movements of the upper limb, the WFFS can quantify the expression of the flexion synergy at the wrist/fingers, if present, as a function of concurrent activity at the shoulder and elbow joints. In doing so, the WFFS can provide additional information with which to speculate about the neural mechanisms underlying stroke-induced movement synergies.

The WFFS is a lightweight, portable device that is attached to the rigid forearm orthosis of the ACT^{3-D} robot [31] (three active DOFs; 0.17m² of horizontal and 0.4 m of vertical workspace). Use of the WFFS in combination with the ACT^{3-D} allows for measurements of wrist/finger forces during any of the tasks in the ACT^{3-D} repertoire, including point-to-point or ballistic reaching, work area, limb perturbations, and simultaneous measurement of shoulder and elbow forces and torques. Arm movements in the ACT^{3-D} can be performed with or without limb support. When supported, the arm rests on a horizontal, frictionless, stiff haptic surface (the “haptic table”). During unsupported movements, the ACT^{3-D} can impose vertical forces on the arm in order to increase or decrease the amount of SABD torque required to lift the limb above the haptic table. Additionally, the WFFS can be adapted easily for use with any robotic device that can incorporate an orthosis similar to that of the ACT^{3-D}.

In order to validate the WFFS, the device was calibrated and used to conduct an experiment showing its force measurement capabilities in chronic hemiparetic stroke. The experiment used the WFFS during a ballistic reaching task, performed while supported and while unsupported, to measure potential torque coupling between the proximal upper limb joints (shoulder and elbow) and the distal upper limb joints (wrist and fingers).

II. REQUIREMENTS

A. ACT^{3-D} Interface

To quantify the potential abnormal coupling between the proximal arm joints and isometric flexion/extension wrist/finger

forces, the proximal joints must be actively loaded. This can be achieved with voluntary movement of the arm in the ACT^{3-D} robot, in which the forearm is placed in a neutral, resting position (full pronation and no ulnar or radial deviation) and secured in a rigid forearm–hand orthosis. Measuring the wrist/finger forces requires a force sensor positioned between the fingers and the orthosis. The required changes to the orthosis to accommodate the WFFS should be lightweight, as any additional mass may affect the measurements made with the ACT^{3-D} robot. Wrist/finger forces must be measurable with both the left and right hand orthoses, and switching the WFFS between the two orthoses should not require more than 10 min. For adaptability to other rehabilitation robots, the changes made to the ACT^{3-D} should be limited to the generic orthosis and should not require modifications to the rest of the robot.

B. Force Measurement

The required force measurement range for the wrist and fingers is from 0 to approximately 450 N. This range is large enough to measure maximum exertions in paretic, nonparetic, and healthy control limbs without losing relevant resolution. To estimate this force range, preliminary maximum flexion measurements were taken using a laboratory force plate with the hands of healthy control subjects in the approximate WFFS configuration. Then, the preliminary results were confirmed in the WFFS with a 445-N load cell. Because all flexion/extension wrist/finger forces must be routed through the force sensor for accurate force recordings, no part of the hand should rest on the orthosis. Measuring finger abduction/adduction forces is outside of the authors’ current research interests and, in that context, would make the WFFS unnecessarily complicated.

In an effort to measure the potential concurrent activity at the thumb, the thumb flexion force must also be measured. This requires an additional (unidirectional) force sensor between the thumb and the orthosis, with force measurement capability ranging from 0 to approximately 100 N (based on preliminary measurements similar to those taken with the wrist/fingers).

C. Ergonomics

In order to accommodate moderately to severely impaired participants who may have limited passive wrist extension, the WFFS must be suitable for a range of hand sizes and cannot require more than 5°–10° of wrist extension. The fingers need to remain in a static, neutral position during the isometric force measurements. Maintaining this position may be difficult for many participants who have a resting flexion bias; therefore, the fingers must be securely but safely restrained. The finger restraint must be comfortable throughout the duration of a recording session.

III. DESIGN

The WFFS consists of a 1-DOF tension–compression load cell (0–445 N capacity, model LC201, Omega Engineering, Stamford, CT) placed through a hole in the forearm orthosis, and secured above and below by mediating mechanisms

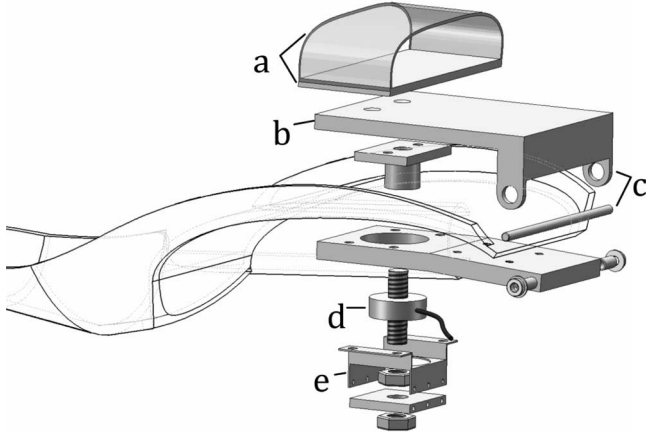


Fig. 1. Schematic of the wrist/finger force sensing module shown on a right hand orthosis from the medial side and expanded to show all components. (a) Thin metal strip and finger strap. (b) Finger plate. (c) Hinged axis. (d) Tension-compression load cell. (e) Alignment mechanism.



Fig. 2. Photograph of the WFFS attached to the ACT^{3-D}. The rigid strap shown on the fingers is secured to the finger plate to restrain the fingers and does not make contact with the orthosis. A similar strap restrains the thumb (not shown).

designed to prevent shear forces on the load cell (see Figs. 1 and 2). The mechanism on top of the load cell consists of a thin, stiff plate [Fig. 1(b)] upon which the fingers rest that is attached on the distal end to a hinge [Fig. 1(c)] with ball bearings. The center axis of the load cell [Fig. 1(d)] is aligned perpendicularly to the hinge. The hinged design ensures correct loading of the force sensor by removing any shear forces due to finger abduction/adduction. The bottom of the load cell is enclosed by an alignment mechanism [Fig. 1(e)] that absorbs shear forces placed on the load cell due to any construction or mounting deviations. The fingers rest on a small, thin, metal strip [Fig. 1(a)] that can be moved along the finger plate to accommodate various hand sizes and then be tightly secured. The metal strip provides a precise point of contact between the fingers and the hinge plate so that measurement of the finger position can be standardized between participants. A finger restraint strap [Fig. 1(a)] made of tough, rigid nylon lined with foam padding, and secured with Velcro is connected to the metal strip to keep the fingers in a neutral position and to prevent slipping into flexion.

Referring to the free-body diagram of the WFFS shown in Fig. 3, the wrist/finger force applied, F_f , is calculated with the

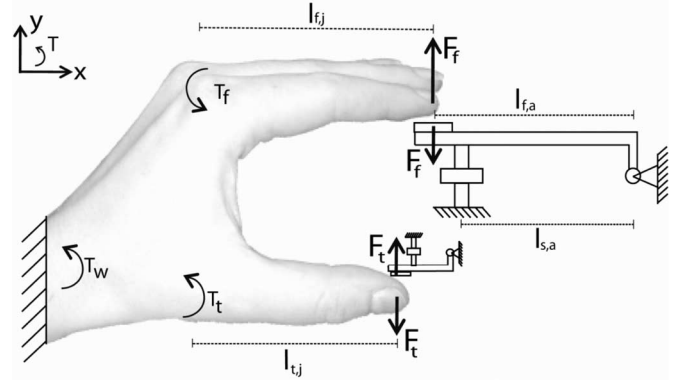


Fig. 3. Free-body diagram of the wrist/finger and thumb components of the WFFS. The thumb component should be rotated slightly about the x -axis (see Fig. 2).

sensor force measured, $F_{f,s}$, and the perpendicular distances from the hinge axis to the finger endpoint and to the sensor, $l_{f,a}$ and $l_{s,a}$, respectively, via

$$F_f = F_{f,s} \left(\frac{l_{s,a}}{l_{f,a}} \right). \quad (1)$$

Using F_f and the distance from the finger endpoint to the finger (metacarpophalangeal) joint axis $l_{f,j}$, the net finger joint torque magnitude T_f is

$$T_f = F_f l_{f,j}. \quad (2)$$

A similar but smaller model of the WFFS was constructed to measure thumb forces (see Fig. 2). The load cell used for the thumb model is a compression load cell (0–111 N capacity, model LC302, Omega Engineering). The thumb force applied, F_t , is calculated similarly to (1), using the thumb sensor force measured, $F_{t,s}$, and the perpendicular distances from the hinge axis to the thumb endpoint and to the thumb sensor, $l_{t,a}$ and $l_{s,a}$, respectively. The magnitude of thumb torque applied is calculated similarly to (2), using F_t and the distance from the thumb endpoint to the thumb (carpometacarpal) joint axis, $l_{t,j}$.

The net wrist torque magnitude is calculated using F_f , F_t , and the distances from the wrist joint axis to the finger and thumb endpoints, $l_{f,w}$ and $l_{t,w}$, respectively

$$T_w = F_f l_{f,w} + F_t l_{t,w}. \quad (3)$$

For all preliminary data collection, raw force signals were low-pass-filtered with the cutoff frequency at 500 Hz (eight-pole analog Butterworth filter; Model 9064, Frequency Devices, Haverhill, MA) to prevent aliasing, then amplified with a gain of 1000, and finally digitized at 1 kHz using an A/D converter.

IV. EXPERIMENTS AND PERFORMANCE

A. Calibration

Two calibrations were performed on the device (Fig. 4). To calibrate the relationship between output voltage and force applied in compression, the device was secured to a wood plate horizontal to the floor, and precision weights were hung from

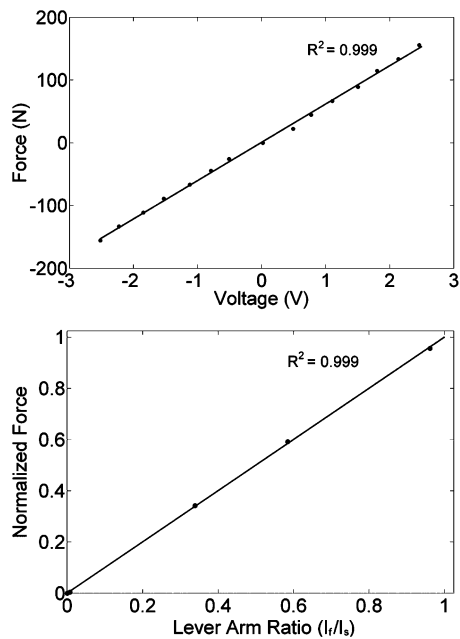


Fig. 4. Calibration curves to verify the linear relationships between (top) voltage and force, and (bottom) lever arm ratio ($l_{f,a}/l_{s,a}$) and normalized force. In the top graph, a positive force indicates compression and a negative force indicates tension.

the top plate by a 16-gauge wire secured in place. The wire was placed over the central axis of the load cell, and the weights hung parallel to the vertical axis of the load cell. For calibrating forces applied in tension, the WFFS was turned over 180°, and the procedure was repeated. To ensure that force measured by the load cell, F_s , was linearly proportional to the lever arm of the applied load, $l_{f,a}$, a precision weight was hung from various positions on the finger plate. Fig. 4 shows the relationship between $l_{f,a}/l_{s,a}$ (lever arm ratio) and force, normalized to the force obtained when $l_{f,a} = l_{s,a}$.

B. Experiments With Stroke Patients

The WFFS was tested with eight individuals with chronic hemiparetic stroke (mean age 62 ± 9 years, range 22–270 months poststroke). All participants had severe to moderate upper limb impairment according to the upper limb Fugl–Meyer motor assessment [32], with scores in the range of 10–37 (mean 20.6) of a possible 66. All had severe to moderate hand impairment according to the Chedoke–McMaster hand assessment [33], with scores ranging from 2 to 5 (mean 2.9) of a possible 7.

Grip force is a common metric in the literature for measuring finger flexion strength [34]–[36]. Prior to experimental testing, grip force was measured in the paretic and nonparetic limbs of all eight participants with a hand dynamometer to ascertain how the forces obtained compared with maximum wrist/finger flexion forces measured with the WFFS. Grip force significantly correlated with the wrist/finger flexion force measured with the WFFS ($r = 0.846$, $p = 0.0001$).

Participants placed the arm in the WFFS-equipped ACT^{3-D} and were tightly secured. They were instructed to move the limb

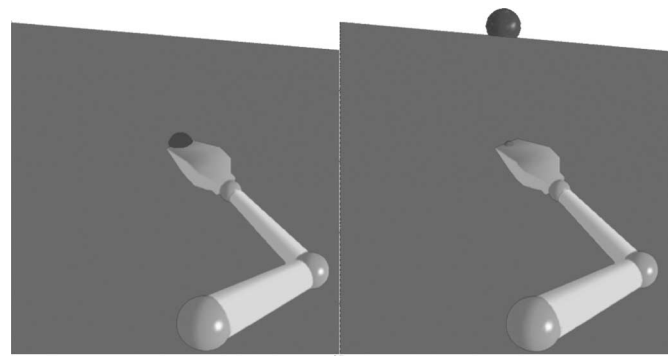


Fig. 5. Visual feedback from the ACT^{3-D} during the task. (Left) Home position. (Right) Reach target.

into a home position of 85° SABD, 90° elbow flexion, and 40° shoulder flexion (adduction in the horizontal plane) and hold for 1 s. Timing and limb positioning were verified using visual feedback on the ACT^{3-D} monitor, which displayed a real-time avatar of the limb [Fig. 5(a)]. After holding the home position for 1 s, a virtual target appeared on the screen, located in the sagittal plane through the virtual shoulder and at a distance equal to the length of the virtual arm [Fig. 5(b)]. Participants were instructed that when the virtual target appeared, they should reach in the horizontal plane as fast and as far as possible toward the target, and hold the maximal reach position for 2 s. Participants were instructed to keep their hand relaxed during the entire trial. The task was performed 11 times while fully supported on the haptically rendered table and was repeated 11 times while unsupported. During the unsupported condition, participants had to generate 50% of their maximum SABD force (as measured in the home position) to lift and maintain the limb above the table. If participants did not maintain the limb above the table, data from these points were excluded from further analysis, and an auditory signal cued them to lift more.

Wrist/finger forces generated during two task windows were selected for analysis: while holding the home position (HOME) and at maximal reach (REACH). Forces were smoothed using a 250-ms moving average filter and were normalized to maximum volitional wrist/finger flexion force. Group results in Fig. 6 show the maximum normalized force generated during each task window. They demonstrate that the wrist/finger flexion forces generated by the paretic limb increased with required SABD force (HOME), and further increased with elbow extension and shoulder flexion (REACH). Forces generated by the thumb followed a similar trend.

Two 3-factor repeated measures analyses of variance (ANOVAs) were used to confirm the effects of limb (paretic, nonparetic), support condition (Table, 50% SAB_{max}), and task (HOME, REACH) on the finger/wrist and thumb flexion forces shown in Fig. 6. A p -value of ≤ 0.05 was considered significant. For the wrist/finger forces, there were significant main effects of limb ($p = 0.0015$), support condition ($p = 0.0016$), and task ($p = 0.0148$), as well as significant interaction effects of limb by support condition ($p = 0.01$) and limb by task ($p = 0.027$). For the thumb forces, there were significant main

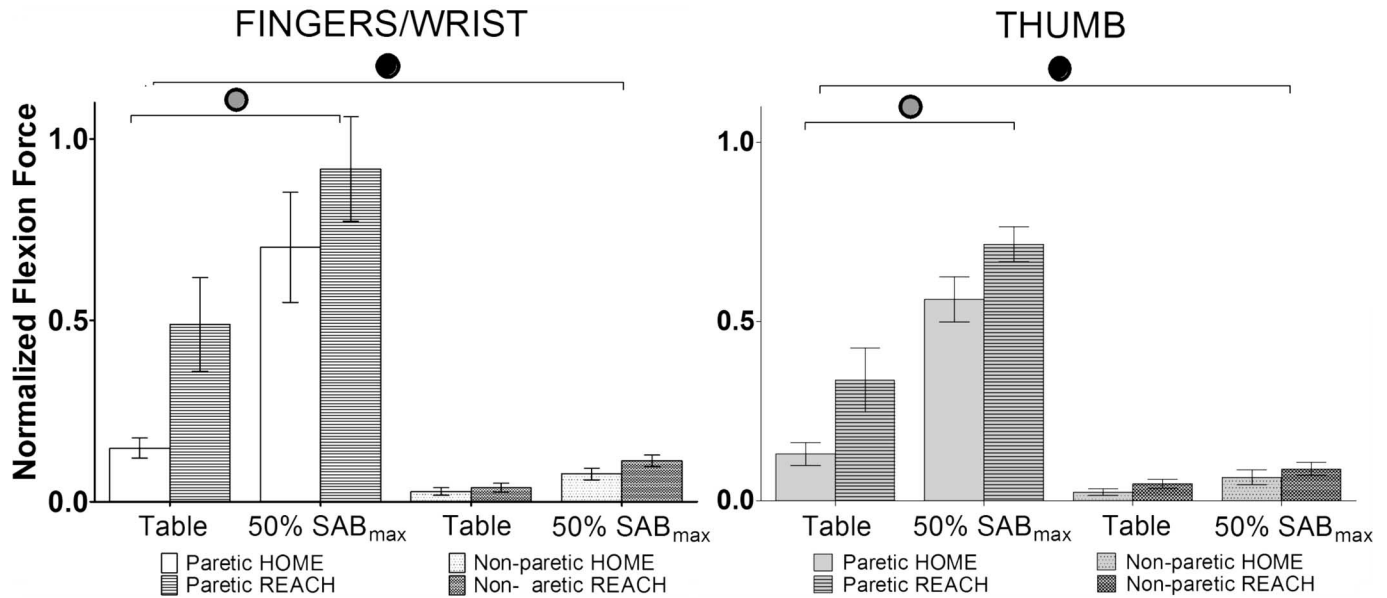


Fig. 6. Mean \pm SEM wrist/finger and thumb forces generated by the paretic and nonparetic limbs in the home position and at maximal reach while fully supported (Table) and while unsupported (having to generate 50% of SAB_{max}). Individual forces were normalized to the maximum volitional flexion force for each participant before taking the group mean. The black circles indicate significant main effects of limb and support condition, and the gray circles indicate a significant main effect of task.

effects of limb ($p < 0.0001$), support condition ($p = 0.0002$), and task ($p = 0.018$), as well as a significant interaction effect of limb by support condition ($p = 0.0005$) and nearly significant interaction effect of limb by task ($p = 0.0528$).

V. DISCUSSION AND CONCLUSION

This letter presents a device designed to measure isometric wrist/finger flexion/extension forces generated during 3-D movements of the paretic upper limb in chronic hemiparetic stroke. The lightweight and portable WFFS can be attached to the distal end of the forearm orthosis of an upper limb robotic device, such as the ACT^{3-D}. Results presented here show that by adding the ability to measure wrist/finger flexion/extension forces to the ACT^{3-D}, the WFFS can quantify abnormal flexion behavior that occurs at the paretic wrist and finger joints during SABD and shoulder flexion/elbow extension tasks.

Studies using robotic devices that focus on the hand and wrist provide an incomplete picture of dysfunction following stroke because they do not consider the abnormal joint torque coupling that occurs when increasing shoulder abductor loading in the paretic upper limb. The quantification of such coupling at the shoulder and elbow joints in both static and dynamic investigative studies [21]–[25] led to the development of a novel robotic-assisted rehabilitative intervention centered on progressive SABD loading [37], [38]. Using the WFFS, this letter shows for the first time that wrist/finger and thumb flexion forces increase drastically as a function of both SABD and shoulder flexion/elbow extension levels. When participants had to generate 50% of their maximum SABD force and then reach out, the wrist/finger flexion forces produced by the paretic hand were near volitional maximum levels ($91.7 \pm 40.8\%$, mean \pm SD).

The implications for these results on hand and wrist rehabilitation can now be considered.

Future research using the WFFS will continue to characterize abnormal coupling at the hand and wrist during 3-D movements and will consider the development of a progressive SABD loading rehabilitation protocol focused on the improvement of hand function. The integration of functional electrical stimulation of forearm extensors will also be investigated, and the WFFS will be used to measure extension forces produced with various stimulation parameters or with stimulation controlled using a brain–computer interface. The WFFS can also be used to study mechanisms of movement disorders that occur in cerebral palsy or following traumatic brain injury.

REFERENCES

- [1] S. Brunnstrom, *Movement Therapy in Hemiplegia: A Neurophysiological Approach*. New York: Harper and Row, 1970.
- [2] T. Twitchell, "The restoration of motor function following hemiplegia in man," *Brain*, vol. 74, pp. 443–480, 1951.
- [3] L. Dovat, O. Lambercy, R. Gassert, T. Maeder, T. Milner, T. C. Leong, and E. Burdet, "HandCARE: A cable-actuated rehabilitation system to train hand function after stroke," *IEEE Trans. Neural Syst. Rehabil. Eng.*, vol. 16, no. 6, pp. 582–591, Dec. 2008.
- [4] M. Bouzit, G. Burdea, G. Popescu, and R. Boian, "The Rutgers Master II—New design force-feedback glove," *IEEE/ASME Trans. Mechatronics*, vol. 7, no. 2, pp. 256–263, Jun. 2002.
- [5] C. D. Takahashi, L. Der-Yeghian, V. H. Le, and S. C. Cramer, "A robotic device for hand motor therapy after stroke," in *Proc. IEEE Int. Conf. Rehabil. Robot. (ICORR)*, 2005, pp. 17–20.
- [6] M. Sivak, C. Mavroidis, and M. Holden, "Design of a low cost multiple user virtual environment for rehabilitation (MUSER) of patients with stroke," *Stud. Health Technol. Inf.*, vol. 142, pp. 319–324, 2009.
- [7] T. Kline, D. G. Kamper, and B. D. Schmit, "Control system for pneumatically controlled glove to assist in grasp activities," in *Proc. IEEE Int. Conf. Rehabil. Robot. (ICORR)*, 2005, pp. 78–81.
- [8] X. Luo, T. Kline, H. Fischer, K. Stubblefield, R. Kenyon, and D. Kamper, "Integration of augmented reality and assistive devices for post-stroke

- hand opening rehabilitation," in *Proc. 27th Annu. Int. Conf. IEEE Eng. Med. Biol. Soc. (EMBC)*, 2005, vol. 7, pp. 6855–6858.
- [9] O. Lambercy, L. Dovat, R. Gassert, E. Burdet, C. Teo, and T. Milner, "A haptic knob for rehabilitation of hand function," *IEEE Trans. Neural Syst. Rehabil. Eng.*, vol. 15, no. 3, pp. 356–366, Sep. 2007.
- [10] D. G. Kamper, B. D. Schmit, and W. Z. Rymer, "Effect of muscle biomechanics on the quantification of spasticity," *Ann. Biomed. Eng.*, vol. 29, no. 12, pp. 1122–1134, 2001.
- [11] S. Li, D. Kamper, and W. Rymer, "Effects of changing wrist positions on finger flexor hypertonia in stroke survivors," *Muscle Nerve*, vol. 33, no. 2, pp. 183–190, 2006.
- [12] D. G. Kamper and W. Z. Rymer, "Impairment of voluntary control of finger motion following stroke: Role of inappropriate muscle coactivation," *Muscle Nerve*, vol. 24, no. 5, pp. 673–681, 2001.
- [13] E. G. Cruz, H. C. Waldinger, and D. G. Kamper, "Kinetic and kinematic workspaces of the index finger following stroke," *Brain*, vol. 128, no. 5, pp. 1112–1121, 2005.
- [14] D. G. Kamper and W. Z. Rymer, "Quantitative features of the stretch response of extrinsic finger muscles in hemiparetic stroke," *Muscle Nerve*, vol. 23, no. 6, pp. 954–961, 2000.
- [15] D. G. Kamper, R. Harvey, S. Suresh, and W. Z. Rymer, "Relative contributions of neural mechanisms versus muscle mechanics in promoting finger extension deficits following stroke," *Muscle Nerve*, vol. 28, no. 3, pp. 309–318, 2003.
- [16] D. G. Kamper, H. C. Fischer, E. G. Cruz, and W. Z. Rymer, "Weakness is the primary contributor to finger impairment in chronic stroke," *Arch. Phys. Med. Rehabil.*, vol. 87, no. 9, pp. 1262–1269, 2006.
- [17] L. Masia, H. Krebs, P. Cappa, and N. Hogan, "Design and characterization of hand module for whole-arm rehabilitation following stroke," *IEEE/ASME Trans. Mechatronics*, vol. 12, no. 4, pp. 399–407, Aug. 2007.
- [18] L. Masia, H. Krebs, P. Cappa, and N. Hogan, "Design, characterization, and impedance limits of hand robot," in *Proc. IEEE Int. Conf. Rehabil. Robot. (ICORR)*, 2007, pp. 1085–1089.
- [19] R. Loureiro and W. Harwin, "Reach & grasp therapy: Design and control of a 9-DOF robotic neuro-rehabilitation system," in *Proc. IEEE Int. Conf. Rehabil. Robot. (ICORR)*, 2007, pp. 757–763.
- [20] R. Beer, J. Dewald, M. Dawson, and W. Rymer, "Target-dependent differences between free and constrained arm movements in chronic hemiparesis," *Exp. Brain Res.*, vol. 156, no. 4, pp. 458–470, 2004.
- [21] T. Sukal, M. Ellis, and J. Dewald, "Shoulder abduction-induced reductions in reaching work area following hemiparetic stroke: Neuroscientific implications," *Exp. Brain Res.*, vol. 176, pp. 594–602, 2007.
- [22] M. Ellis, T. Sukal, T. DeMott, and J. Dewald, "Augmenting clinical evaluation of hemiparetic arm movement with a laboratory-based quantitative measurement of kinematics as a function of limb loading," *Neurorehabil. Neural Repair*, vol. 22, pp. 321–329, 2008.
- [23] R. Beer, J. Given, and J. Dewald, "Task-dependent weakness at the elbow in patients with hemiparesis," *Arch. Phys. Med. Rehabil.*, vol. 80, no. 7, pp. 766–772, 1999.
- [24] J. Dewald and R. Beer, "Abnormal joint torque patterns in the paretic upper limb of subjects with hemiparesis," *Muscle Nerve*, vol. 24, pp. 273–283, 2001.
- [25] M. Ellis, A. Acosta, J. Yao, and J. Dewald, "Position-dependent torque coupling and associated muscle activation in the hemiparetic upper extremity," *Exp. Brain Res.*, vol. 176, pp. 594–602, 2007.
- [26] R. Beer, M. Ellis, B. Holubar, and J. Dewald, "Impact of gravity loading on post-stroke reaching and its relationship to weakness," *Muscle Nerve*, vol. 36, no. 2, pp. 242–250, 2007.
- [27] R. F. Beer, J. P. Dewald, M. L. Dawson, and W. Z. Rymer, "Target-dependent differences between free and constrained arm movements in chronic hemiparesis," *Exp. Brain Res.*, vol. 156, pp. 458–470, 2004.
- [28] R. F. Beer, M. D. Ellis, B. G. Holubar, and J. P. A. Dewald, "Impact of gravity loading on post-stroke reaching and its relationship to weakness," *Muscle Nerve*, vol. 36, no. 2, pp. 242–250, 2007.
- [29] J. McPherson, M. Ellis, C. Heckman, and J. Dewald, "Evidence for increased activation of persistent inward currents in individuals with chronic hemiparetic stroke," *J. Neurophysiol.*, vol. 100, pp. 3236–3243, 2008.
- [30] J. Dewald, R. Beer, J. Given, J. McGuire, and W. Z. Rymer, "Reorganization of flexion reflexes in the upper extremity of hemiparetic subjects," *Muscle Nerve*, vol. 22, pp. 1209–1221, 1999.
- [31] T. Sukal, M. Ellis, and J. Dewald, "Use of a novel robotic system for quantification of upper limb work area following stroke," in *Proc. 27th Annu. Int. Conf. IEEE Eng. Med. Biol. Soc. (EMBC)*, 2005, pp. 5032–5035.
- [32] A. Fugl-Meyer, L. Jaasko, I. Leyman, S. Olsson, and S. Steglind, "The post-stroke hemiplegic patient. 1. A method for evaluation of physical performance," *Scand. J. Rehabil. Med.*, vol. 7, pp. 13–31, 1975.
- [33] C. Gowland, P. Stratford, M. Ward, J. Moreland, W. Torresin, S. Van Hulleenaar, J. Sanford, S. Barreca, B. Vanspall, and N. Plews, "Measuring physical impairment and disability with the Chedoke-McMaster stroke assessment," *Stroke*, vol. 24, no. 1, pp. 58–63, 1993.
- [34] A. Hamilton, R. Balnave, and R. Adams, "Grip strength testing reliability," *J. Hand Ther.*, vol. 7, pp. 163–179, 1994.
- [35] L. Jones, "The assessment of hand function: A critical review of techniques," *J. Hand Surg. Amer.*, vol. 14, pp. 221–228, 1989.
- [36] V. Mathiowetz, N. Kashman, G. Volland, K. Weber, M. Dowe, and S. Rogers, "Grip and pinch strength: Normative data for adults," *Arch. Phys. Med. Rehabil.*, vol. 66, pp. 69–74, 1985.
- [37] M. Ellis, T. Sukal-Moulton, and J. Dewald, "Targeted 3-D robotic intervention improves upper extremity work area in chronic stroke: Targeting abnormal joint torque coupling with progressive shoulder abduction loading," *IEEE Trans. Robot.*, vol. 25, no. 3, pp. 549–555, Mar. 2009.
- [38] M. D. Ellis, T. Sukal-Moulton, and J. P. A. Dewald, "Progressive shoulder abduction loading is a crucial element of arm rehabilitation in chronic stroke," *Neurorehabil. Neural Repair*, May 2009, DOI: 0:1545968309332927.